JOURNAL OF RESEARCH of the National Bureau of Standards—A. Physics and Chemistry
Vol. 75A, No. 3, May–June 1971

Optical and Mechanical Properties of Some Neodymium-Doped Laser Glasses*

R. M. Waxler, G. W. Cleek, I. H. Malitson, M. J. Dodge, and T. A. Hahn

Institute for Materials Research, National Bureau of Standards, Washington, D.C. 20234

(January 22, 1971)

Studies have been made to evaluate thermo-optic and piezo-optic properties of five laser glasses. Measurements were made at the Cd red line, $\lambda = 0.6438$ μm, over a wide range of temperatures and pressures using interferometric and polarimetric techniques. The refractive index-temperature data show both positive and negative values and small changes with temperature. The changes in index with applied compressive stress are positive in value. Other optical properties evaluated were homogeneity, transmittance, and refractive index as a function of wavelength. An ultrasonic pulse-echo technique was used to determine the elastic constants, Young's modulus, shear modulus, bulk modulus, and Poisson's ratio. Data for thermal expansion, thermal conductivity, density, hardness and chemical composition are also given. Calculations were made of the thermal change of refractive index at constant volume. These data can be used to calculate corrections for the distortions of the wavefront of light generated in lasers.

Key words: Chemical composition; density; glasses; hardness; laser; optical homogeneity; photoelasticity; refractive index; thermal conductivity; thermo-optic properties; transmittance.

1. Introduction

When a glass laser is operated, thermal effects produce optical distortions which virtually preclude diffraction-limited operation even if the materials themselves are of diffraction-limited quality [1].[1] The changes in optical pathlength induced by optical pumping of neodymium-doped glass rods have been studied by several investigators [2–8]. This overall change is caused by changes in certain parameters; thermal expansion alters the physical dimensions of the cavity, and the refractive index varies as a function of the local temperature and stress. Data on these properties are needed to calculate the corrections for the distortion of the wavefront.

Several mechanisms have been proposed in the literature to account for the damage observed in laser materials operated at high power levels [9–12]. These can be properly assessed only when data on the material properties are known.

Compilations of data on the properties of laser materials have been published [13–14], but these are not complete. For the purposes mentioned above, data are presented in this paper on thermal expansion, the elastic constants and the change in refractive index as a function of temperature and stress. Included also are original data on the important laser properties; optical quality, transmittance, refractive index, thermal conductivity, hardness, density, and chemical composition. Measurements were made on specimens of five commercially made neodymium-doped laser glasses, and, for purposes of identification, these have been designed as glasses A, B, C, D, and E.

2. Optical Quality

Each specimen was examined to be sure that the glass contained no gross inhomogeneities, and that the specimen was well annealed. Inclusions and seeds were found by illuminating with a beam of light from the side and viewing normally against a dark background [15]. The optical homogeneity was determined from shadowgraphs and interferograms [16]. The state of anneal was ascertained by measuring the strain birefringence with a sensitive tint plate when the specimen was placed between crossed polarizers [17].

Specimen A was in the form of a cylinder 8 cm in diameter and 2.9 cm thick. Three inclusions that appeared to be metallic and two seeds were found. The specimen was annealed, and the birefringence was reduced to a negligible value except for the very edge of the specimen where a residual path difference of 2 nm/cm remained. The interferogram and shadowgraph are shown in figures 1a and 1b, respectively.

Specimen B, which was cut from a finished oscillator rod, had no seeds or inclusions. It was 5.5 cm

*The work described in this report was sponsored by the Advance Research Projects Agency, Department of Defense.

[1] Figures in brackets indicate the literature references at the end of this paper.

long and 1.6 cm in diameter. The specimen appeared to be well annealed, so that no further heat treatment was considered necessary. The interferogram and shadowgraph are shown in figures 2a and 2b, respectively.

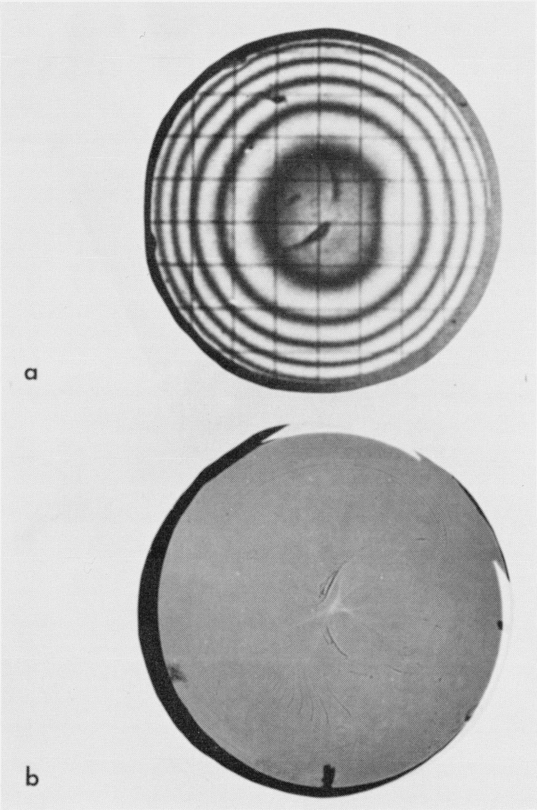

FIGURE 1. (a) *Twyman-Green interferogram of laser glass specimen A;* (b) *shadowgraph of laser glass specimen A.*

Specimens C and D were in the form of rectangular blocks about 4.5 cm × 1 cm × 1 cm. No seeds or inclusions were observed, and the glasses appeared to be well-annealed. The specimens were too small for meaningful interferograms so that only shadowgraphs were taken. The shadowgraph of specimen C is shown in figure 3a and that of specimen D is shown in figure 3b.

Specimen E was in the form of a cylinder 15.2 cm long and 2.5 cm in diameter. There were no seeds or inclusions, and the specimen was well-annealed. The interferogram and shadowgraph are shown in figure 4a and b, respectively.

From the striae that can be observed in the five shadowgraphs, it was concluded that all of the glasses could be regarded as Grade B,[2] or better, according to the military specification for optical glass [15]. The absence of abrupt changes in the fringe pattern of the interferogram was a confirmation that there

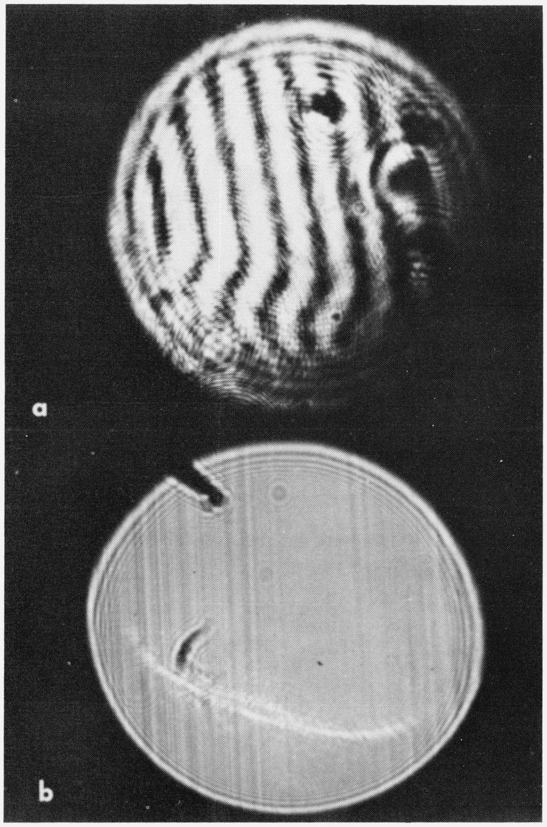

FIGURE 2. (a) *Twyman-Green interferogram of laser glass specimen B;* (b) *shadowgraph of laser glass specimen B.*

were no gross inhomogeneities present. From specimens A through E smaller samples were cut for the various studies of this report.

3. Transmittance

Transmittance curves for neodymium-doped silicate laser glasses have been published [14]. Since only very small variations are found for the different silicate glasses, the transmittance curve for a sample of specimen A is shown in figure 5 as a typical example. The transmittance was measured on a commercial double beam spectrophotometer.

4. Refractive Index

The glass specimens ground and polished for refractive index studies were either in the form of prisms or cuboids.[3] The two prisms had faces approximately 2 cm square and refracting angles near 60° (see table 2). These specimens were measured by means of the classical minimum deviation method using two spectrometers shown schematically in figure 6. The spec-

[2] In reference [15], Grade B glass is defined as glass which contains only striae that are light and scattered when viewed in the direction of maximum visibility when tested by the specified methods.

[3] Specimens B, C, and D were in the form of cuboids because there was insufficient material for prisms.

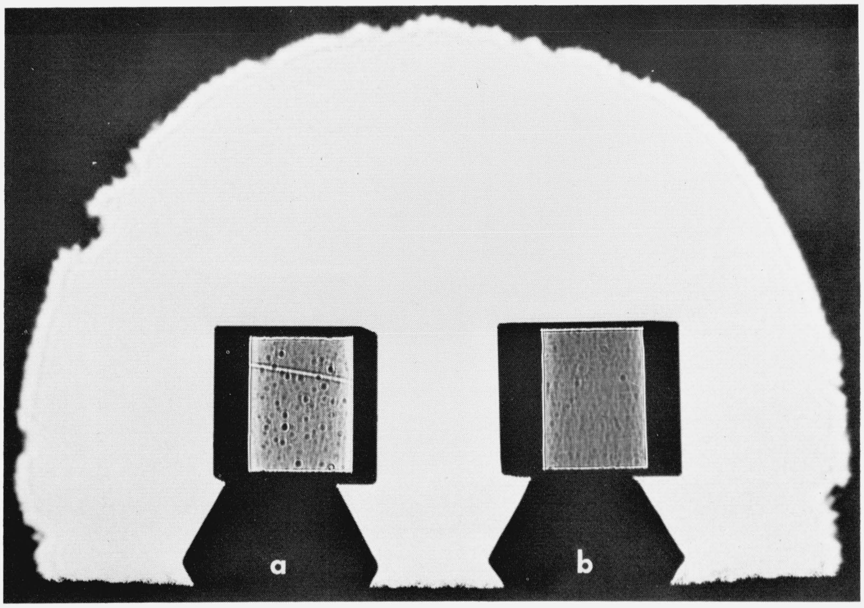

FIGURE 3. (a) *Shadowgraph of laser glass specimen C;* (b) *shadowgraph of laser glass specimen D.*

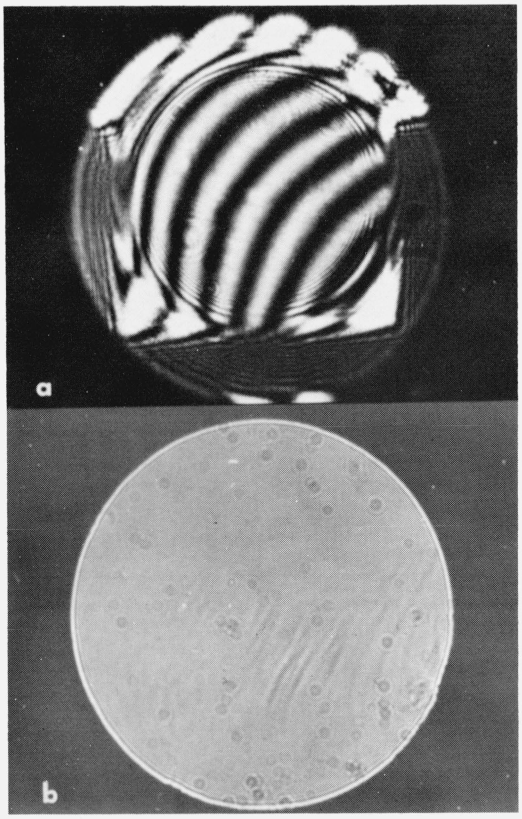

FIGURE 4. (a) *Twyman-Green interferogram of laser glass specimen E;* (b) *shadowgraph of laser glass specimen E.*

trometer shown in Figure 6a is designed for visible-region refractometry. When an infrared image converter is set at the viewing end of the telescope, visual sighting is extended to about 1.1 μm in the near infrared. The spectrometer outlined in figure 6b employs mirror optics and is used for nonvisible-region refractometry. Both instruments and procedures for high-precision refractive index measurements have been described in previous publications [18, 19, 20].

The technique employed for the refractive index measurements of the cuboids was somewhat novel and has been reported in an earlier publication [21]. Briefly, a specimen was optically contacted to a dense flint-glass prism of known refractive index as shown in figure 7. The visual spectrometer (fig. 6a) was used to measure the angles describing the optical path through the combination. Ray tracing equations were derived to compute the refractive index. Index measurements for the five specimens were made at selected wavelengths from 0.4 to 2.3 μm for the prominent emission spectra of mercury, cadmium, and helium at a controlled room temperature near 20 °C.

The indices of refraction of these glasses were represented by a modified Herzberger dispersion equation [22] of the form

$$n = A + BL + D\lambda^2 + E\lambda^4 \qquad (1)$$

where $L = \dfrac{1}{\lambda^2 - C}$ and where λ is expressed in micrometers, μm. The parameters for each glass are given

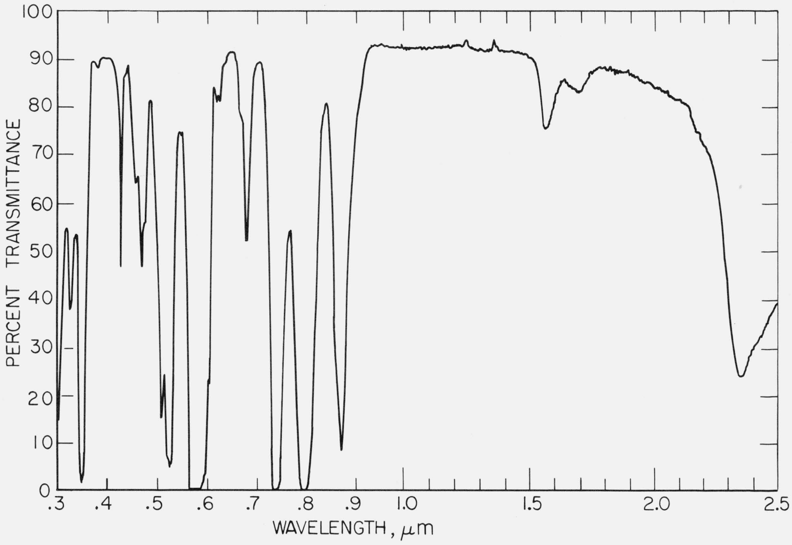

FIGURE 5. *Transmittance curve for laser glass specimen A, 1.882 cm thick.*

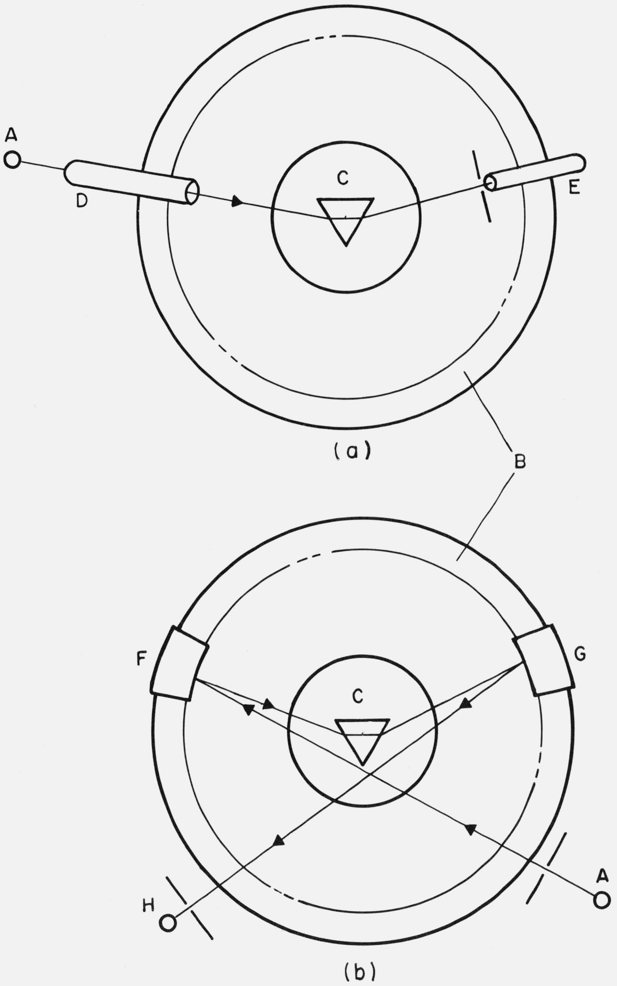

FIGURE 6. (a) *Schematic of spectrometer used for visible-region refractometry. A, source; B, divided circle; C, prism table; D, collimator; E, telescope;* (b) *schematic of spectrometer used for nonvisible-region refractometry. A, source; B, divided circle; C, prism table; F, collimating mirror (fixed): G, movable mirror; H, detector.*

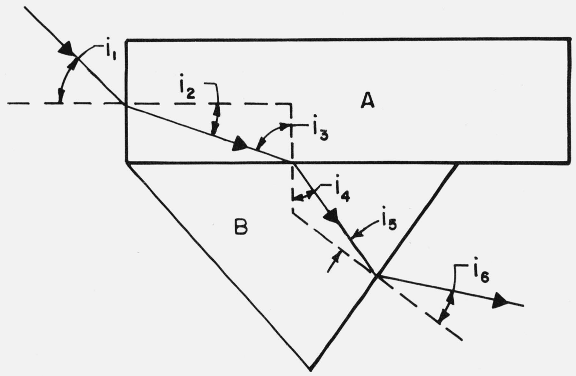

FIGURE 7. *Cuboid-prism combination showing the optical path and angles of refraction. A, Neodymium-doped glass specimen; B, dense flint glass prism.*

in table 1 and were obtained by an iterative process carried out on a time-sharing computer. Each step of iteration consisted of the solving of a set of linear equations.

The original Herzberger equation assigns a fixed value of 0.028 to the parameter C, and consists of five terms which includes a term in L^2. This term in L^2 is also initially included in this modified form, but

TABLE 1. *Parameters of dispersion equations for neodymium-doped laser glasses at 20 °C*

$$n = A + \frac{B}{\lambda^2 - C} + D\lambda^2 + E\lambda^4$$

Parameter	Glass A	Glass B	Glass C	Glass D	Glass E
A	1.507837	1.513668	1.505575	1.509685	1.555067
B	0.003966	0.003812	0.003990	0.003919	0.004406
C	.013919	.017734	.015085	.019009	.012773
D	−.002659	−.005700	−.002919	−.004748	−.002963
E	−.000020	.001510	.000103	.001084	−.000025

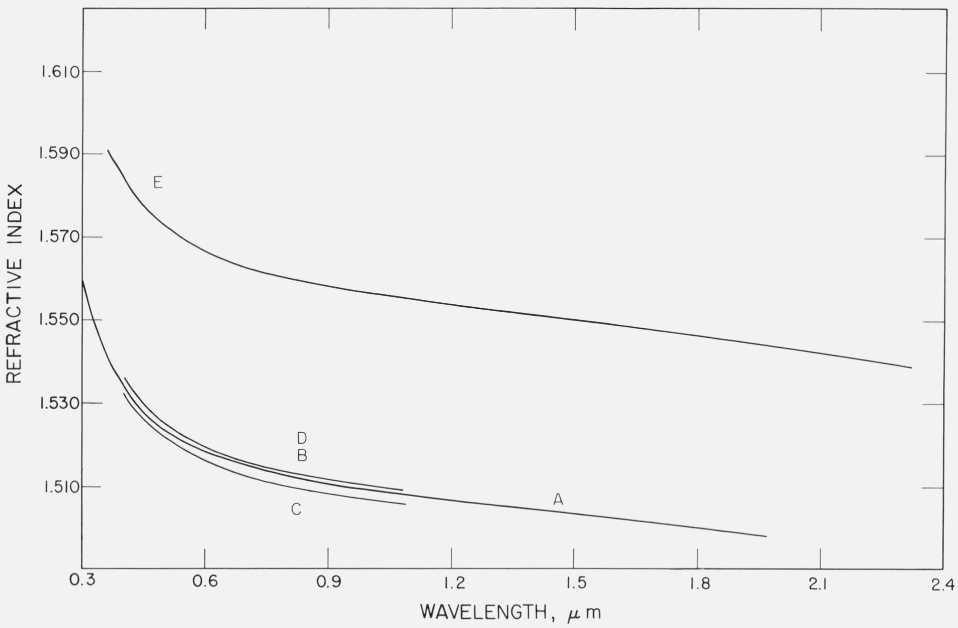

FIGURE 8. *Refractive index of neodymium-doped laser glasses.*

serves only to simplify our adjustment of the parameter C which enters into the formula nonlinearly. The L^2 term drops out of the final equation for relatively small sets of data, as is the case in these experiments, where the wavelength range is primarily over the visible and near-infrared regions of the spectrum.

The average absolute residuals of index for these glasses were from 5 to 10×10^{-6}. The maximum residual, as much as 3×10^{-5}, was obtained at $\lambda = 0.5876$ μm where there is observational uncertainty because of the proximity of this line to a strong absorption band of neodymium. The computed values of index are listed in table 2 and plotted as a function of wavelength in figure 8 (glasses designated B and D are represented by the same curve for sake of clarity). The refractive index at any specific wavelength intermediate to those listed in the table for each glass may be interpolated to five decimal places by means of the dispersion equations.

TABLE 2. *Computed refractive indices of neodymium-doped laser glasses at 20 °C*

Wave-length (μm)	Spectral source	Glass [a] A	Glass [b] B	Glass [b] C	Glass [b] D	Glass [a] E
0.30215	Hg	1.55884				
.334148	Hg	1.54811				
.340365	Cd	1.54643				
.346693	Cd	1.54483				
.361248	Cd	1.54150				
.365015	Hg	1.54072				1.59125
.404656	Hg	1.53387	1.53888	1.53194	1.53601	1.58376
.435835	Hg	1.52986	1.53479	1.52784	1.53175	1.57937
.467816	Cd	1.52660		1.52452	1.52831	1.57580
.479991	Cd	1.52554	1.53036	1.52344	1.52719	1.57463
.508582	Cd	1.52335		1.52121	1.52488	1.57222
.546074	Hg	1.52099	1.52568	1.51881	1.52240	1.56962
.587561	He	1.51889	1.52354	1.51667	1.52019	1.56729
.643847	Cd	1.51663	1.52116	1.51437	1.51781	1.56480
.667815	He	1.51582		1.51356	1.51696	1.56391
.706519	He	1.51468	1.51912			1.56264
1.01398	Hg	1.50899		1.50662	1.50983	1.55633
1.08297	He	1.50811	1.51235	1.50574	1.50900	1.55536
1.12866	Hg	1.50756				1.55475
1.3622	Hg					1.55187
1.39506	Hg	1.50464				1.55148
1.52952	Hg	1.50321				1.54989
1.6932	Hg	1.50144				1.54791
1.7092	Hg	1.50126				1.54771
1.81307	Hg	1.50009				1.54640
1.97009	Hg	1.49823				1.54433
2.32542	Hg					1.53913

[a] Prism. [b] Cuboid.

5. Thermal Expansion and Thermal Change in Refractive Index

The thermal expansion and the thermal change in refractive index were determined simultaneously by an interferometric method using collimated monochromatic light. The apparatus, described by Saunders [23], records localized Fizeau-type fringes on film. The interferometer assembly is shown in figure 9.

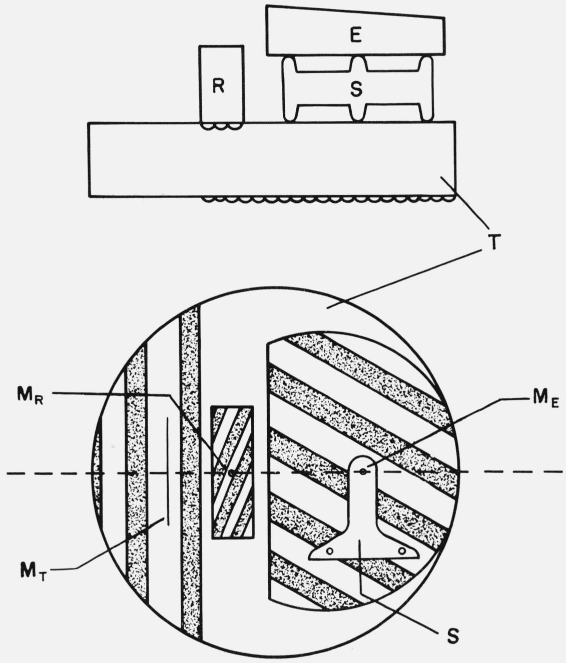

FIGURE 9. *Interferometer assembly for the measurement of thermal expansion and thermal change in refractive index.*

E, an interferometer plate; S, thermal expansion specimen; R, refractive index specimen; T, interference thermometer; M_E, M_R, and M_T, reference lines for the interference fringes of thermal expansion, refractive index change and temperature change.

The set of fringes on the left are obtained between the top and bottom surfaces of the lower fused silica plate, T, and are calibrated in terms of temperature so that they serve as an optical thermometer. The center set of fringes are obtained between the top and bottom surfaces of the index sample, R, and are used to calculate the change in refractive index. Beneath this sample is a frosted area on the lower plate so that no fringes are formed at the interface. The third set of fringes are formed by the slight wedge introduced between the upper plate, E, and the lower plate, T, when they are separated by the expansion sample, S, which is cut from the same material as the index sample, R. These fringes are used to obtain the thermal expansion. The assembly is heated by a vertical tube furnace and the shift in the three sets of fringes are recorded simultaneously on a single strip of 35 mm film as a function of temperature.

The interference pattern generated by the sample of thickness, t, and refractive index, n, is expressed by the equation,

$$N\lambda = 2nt \tag{2}$$

which relates the optical path, nt, and the fringe number, N, when monochromatic light of wavelength, λ, passes twice through the sample at normal incidence. By differentiating with respect to temperature, T, and rearranging, it is found that

$$\frac{\Delta n}{\Delta T} = \frac{\lambda \Delta N}{2t\Delta T} - \frac{n\Delta t}{t\Delta T}. \tag{3}$$

A measurement of the number of fringes that pass a point of reference, and the change in t together with data on the initial index and the temperature interval, permits the calculation of the change in refractive index as a function of temperature [24].

In this experiment, the glass samples were approximately 0.5 cm in thickness. Measurements were made at temperature intervals of about 50 °C using cadmium red radiation, $\lambda = 0.6438$ μm. The recorded fringe shifts from the expansion samples were counted and values of $\Delta t/t$ were calculated. From the recorded fringe shifts of the index samples and the values of $\Delta t/t$, calculations of the values of Δn were made by

TABLE 3. *Increase in length per unit length,* $\Delta t/t$, *as a function of temperature*

Temperature °C	Laser Glasses				
	A	B	C	D	E
0	0.0×10^{-4}	0.0×10^{-4}	0.0×10^{-4}	0.0×10^{-4}	0.0×10^{-4}
10	1.0	1.0	.8	.9	.8
20	1.9	1.9	1.7	1.9	1.6
30	2.9	2.9	2.6	2.9	2.5
40	3.9	4.0	3.5	3.8	3.3
50	4.9	5.0	4.4	4.8	4.2
60	5.9	6.1	5.4	5.8	5.1
70	6.9	7.2	6.4	6.8	6.0
80	7.9	8.3	7.4	7.9	6.9
90	9.0	9.4	8.4	8.9	7.9
100	10.0	10.6	9.4	9.9	8.8
110	11.0	11.8	10.5	11.0	9.8
120	12.1	13.0	11.6	12.1	10.8
130	13.1	14.2	12.7	13.1	11.8
140	14.2	15.4	13.8	14.2	12.8
150	15.2	16.6	14.9	15.3	13.8
160	16.3	17.8	16.0	16.4	14.8
160	17.4	19.1	17.1	17.5	15.9
180	18.4	20.4	18.3	18.6	16.9
190	19.5	21.6	19.4	19.7	18.0
200	20.6	22.9	20.6	20.8	19.0
210	21.6	24.2	21.7	21.9	20.1
220	22.7	25.4	22.9	23.0	21.1
230	23.8	26.7	24.0	24.1	22.2
240	24.9	28.0	25.2	25.2	23.3
250	25.9	29.3	26.3	26.4	24.4
260	27.0	30.6	27.5	27.5	25.5
270	28.1	31.8	28.6	28.6	26.5
280	29.1	33.1	29.7	29.7	27.6
290	30.2	34.4	30.8	30.8	28.7
300	31.3	35.6	32.0	32.0	29.8

TABLE 4. *Change in refractive index, (Δn), as a function of temperature at 0.6438 μm*

Temperature °C	Laser Glasses A	B	C	D	E
0	0.0×10^{-4}	0.0×10^{-4}	0.0×10^{-4}	0.0×10^{-4}	0.0×10^{-4}
10	−.2	−.2	.0	−.5	.3
10	−.4	−.3	.0	−.9	.5
30	−.6	−.5	−.1	−1.3	.8
40	−.8	−.7	−.1	−1.7	1.1
50	−.9	−.8	−.2	−2.0	1.4
60	−1.0	−1.0	−.2	−2.3	1.7
70	−1.1	−1.2	−.3	−2.6	2.0
80	−1.2	−1.3	−.3	−2.8	2.3
90	−1.2	−1.5	−.4	−3.0	2.6
100	−1.3	−1.7	−.5	−3.2	2.9
110	−1.3	−1.9	−.5	−3.4	3.2
120	−1.3	−2.0	−.6	−3.5	3.6
130	−1.2	−2.2	−.6	−3.6	3.9
140	−1.2	−2.4	−.7	−3.7	4.3
150	−1.1	−2.5	−.7	−3.7	4.7
160	−1.1	−2.7	−.8	−3.8	5.0
170	−1.0	−2.8	−.8	−3.8	5.5
180	−.9	−3.0	−.8	−3.8	5.9
190	−.7	−3.1	−.8	−3.7	6.3
200	−.6	−3.3	−.9	−3.7	6.8
210	−.4	−3.4	−.8	−3.6	7.2
220	−.2	−3.6	−.8	−3.6	7.7
230	−.1	−3.7	−.8	−3.5	8.2
240	.1	−3.8	−.7	−3.4	8.8
250	.4	−3.9	−.7	−3.3	9.3
260	.6	−4.0	−.6	−3.1	9.9
270	.8	−4.1	−.5	−3.0	10.5
280	1.1	−4.2	−.3	−2.8	11.1
290	1.4	−4.3	−.2	−2.7	11.7
300	1.6	−4.3	0.0	−2.5	12.4

means of eq (3). The data were fitted by computer to a cubic equation and values of both $\Delta t/t$ and Δn at temperature intervals of 10 °C were obtained. Values of thermal expansion and change in refractive index for the five glasses are given from 0 to 300 °C in tables 3 and 4. Guided by the theory of dispersion for dn/dT in solids [25, 26], it has been assumed that the values of dn/dt are very close at the wavelengths of 0.6438 μm and 1.06 μm, the lasing wavelength of neodymium-doped glasses.

It was estimated that shifts could be measured to one-tenth of an interference fringe. Calculations showed that the sensitivity of measurement of $\Delta t/t$ and Δn were within 0.05×10^{-4} and 0.2×10^{-4}, respectively. The standard deviation for each value of $\Delta t/t$ and Δn was found to be within 0.2×10^{-4}.

6. Photoelastic Constants

When a uniaxial stress is applied to a specimen of glass of refractive index, n, there is a change in refractive index, Δn_1, for polarization along the line of stress and another change, Δn_2, for polarization perpendicular to the stress direction [24]. The two changes are related to the change in stress, ΔP, by the equations,

$$\Delta n_1=\frac{n^3}{2}\,[q_{11}]\Delta P \tag{4}$$

and

$$\Delta n_2=\frac{n^3}{2}\,[q_{12}]\Delta P, \tag{5}$$

where the q_{ij} are known as the piezo-optic constants. There are corresponding relationships between the state of strain existing in the glass and changes in the refractive index and, in this case, the constants are called the elasto-optic constants, p_{ij}. The p_{ij} are given by

$$p_{11}=C_{11}q_{11}+2C_{12}q_{12} \tag{6}$$

and

$$p_{12}=C_{11}q_{12}+C_{12}(q_{11}+q_{12}), \tag{7}$$

where the C_{ij} are the elastic constants.

The piezo-optic constants of a neodymium-doped laser glass have been determined from the optical path difference introduced into a specimen by uniaxial stress and the equation,

$$(\Delta n_2-\Delta n_1)=\frac{n^3}{2}\,[q_{12}-q_{11}]\Delta P, \tag{8}$$

in combination with the measured change in index from applied hydrostatic pressure, and the equation

$$\Delta n=\frac{n^3}{2}\,[q_{11}+2q_{12}]\Delta P. \tag{9}$$

The elasto-optic constants were then evaluated by using eqs (6) and (7). The studies were made using the cadmium red line at 0.6438 μm.

6.1. Hydrostatic Pressure

In this experiment localized interference fringes were observed in a plate of the glass approximately 1 cm × 1 cm × 0.5 cm which had plane, polished, nearly parallel faces. The fringes were viewed in reflection using collimated light at normal incidence. Equation (2) still applies. Application of hydrostatic pressure will cause a shift in the interference fringes, because of the changes induced in n and t. By differentiating eq (2) with respect to pressure and rearranging, it is found that

$$\frac{\Delta n}{\Delta P}=\frac{\Delta N\lambda}{2t\Delta P}-\frac{n\Delta t}{t\Delta P}. \tag{10}$$

A measurement of the number of fringes that pass a point of reference, and the thickness together with data on the initial index and the linear compression, $\Delta t/t$, permits calculation of the change in index [27].

The specimen was immersed in oil in a pressure vessel equipped with glass windows. Hydrostatic pressure was generated by compressing the liquid, and the number of interference fringes passing a fixed reference mark was determined visually. The specimen was subjected to a maximum pressure of about 1×10^8 N/m^2 and the pressure was measured with a Heise pressure gauge.

6.2. Uniaxial Loading

A specimen in the form of a parallelepiped with dimensions approximately 1 cm$\times$1 cm$\times$3 cm was subjected to uniform compression along the long dimension. The specimen was placed in a 45 degree position between crossed polarizers, and the relative retardation introduced between the light rays with electric vectors parallel and perpendicular to the direction of stress was measured with a Babinet-Soliel compensator. The induced birefringence can be related to the induced optical path difference by

$$\frac{(\Delta n_2 - \Delta n_1)}{\Delta P} = \frac{(\Delta N_2 - \Delta N_1)\lambda}{t\Delta P} \tag{11}$$

where ΔN_1 and ΔN_2 are respectively the changes in fringe number parallel and perpendicular to the direction of stress.

A loading frame was used where a yoke with suspended weights brings a piston to bear on the specimen [28]. To insure uniformity of loading, steel caps were machined to fit over the specimen at either end. A small depression was machined in the center of each cap to accommodate a steel ball where the load was applied. Similar depressions were machined at the end of the piston and on the loading frame where the specimen rested. Six calibrated fifty pound weights were used so that the total load was three hundred pounds. The compressive stress on the sample was about 0.13×10^8 N/m^2. Information was also obtained on the effect of wavelength variation upon the stress-induced birefringence. Apparatus which included a continuous light source, a monochromator and a pull rod with a lever arm for exerting stress upon the specimen was employed [29]. In this way data on $(q_{12} - q_{11})$ from 0.300 μm to 1.300 μm were obtained (see fig. 10).

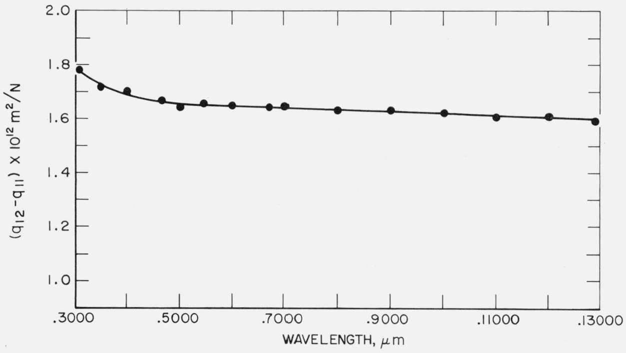

FIGURE 10. *Difference in the piezo-optic constants of laser glass specimen A as a function of wavelength.*

6.3. Results

The q_{ij} and p_{ij} which were evaluated from the data are reported in table 5. The constants obtained for these neodymium-doped laser glasses seem to be in conformity with other reported values for silica-based optical glasses [30]. The relative stress optical coefficient, C, an often used parameter is defined as

$$C = \frac{n^3}{2}(q_{12} - q_{11}).$$

In the experiments involving the relative change in optical path the accuracy is 1 percent or better. In determining the absolute change in optical path with applied hydrostatic pressure, duplicate measurements agreed to within 0.1 interference fringe. However, in this case, the major portion of the path change is due to change in thickness of the specimen which is calculated from the elastic constants (see following section). These latter values are estimated to have an accuracy of $\pm$ 2 percent, so the values of the photoelastic constants reported in table 5 can be no better than this.

In figure 10, it can be seen that $(q_{12} - q_{11})$ is nearly constant over an extended wavelength range with a slight rise near the absorption edge. This fact has a bearing upon whether the data measured at 0.6438 μm pertain at the lasing wavelength of 1.060 μm (see sec. 5). There are no data in the literature on the absolute values of the photoelastic constants of any material in this region. It is assumed here that absolute values of the constants at the two wavelengths are very close.

TABLE 5. *The photoelastic constants of neodymium-doped laser glasses*

Glass	q_{11}	q_{12}	p_{11}	p_{12}
	$\times 10^{12} m^2/N$			
A	0.53	2.16	0.134	0.225
B	.54	2.04	.139	.218
C	.58	2.18	.139	.222
D	.78	2.36	.153	.232
E	.12	1.21	.105	.184

7. Elastic Constants

The elastic constants were determined by an ultrasonic pulse-echo technique [31]. Pulses with a frequency of 14 MHz and a duration of 0.5 to 1.0 μs produced by a pulsed oscillator, were passed through an attenuator to a quartz transducer to which the specimen was coupled with resin 276-V9. Signals representing the first transit and subsequent echoes from a second quartz transducer on the opposite end of the specimen were amplified with a wideband amplifier, and transit times were determined by an oscilloscope with a dual trace unit which also displayed the input pulse.

Elastic moduli were calculated from the following equations:

$$\text{Young's; modulus, } E=\rho V_T^2\left(\frac{3V_L^2-4V_T^2}{V_L^2-V_T^2}\right) \tag{12}$$

$$\text{Shear modulus, } G=\rho V_T^2 \tag{13}$$

$$\text{Bulk modulus, } K=\rho\,\frac{(3V_L^2-4V_T^2)}{3} \tag{14}$$

$$\text{Poisson's ratio, } \gamma=\frac{V_L^2-2V_T^2}{2(V_L^2-V_T^2)} \tag{15}$$

where V_T=transverse wave velocity, and V_L=longitudinal wave velocity.

The measured values for the five glasses are listed in table 6. These values are estimated to be reproducible to ±2 percent.

TABLE 6. *Elastic Constants of Neodymium-Doped Laser Glasses*

	Glass				
	A	B	C	D	E
Young's Modulus, E	6.81×10^{10}N/m^2	6.58×10^{10}N/m^2	6.41×10^{10}N/m^2	6.15×10^{10}N/m^2	9.08×10^{10}N/m^2
Shear Modulus, G	2.79	2.66	2.61	2.51	3.62
Bulk Modulus, K	4.03	4.16	3.94	3.75	6.14
Poisson's Ratio, γ	0.218	0.236	0.229	0.226	0.255

8. Self-Focusing Induced by Temperature Change and Electrostriction

The measurements of the change of refractive index with temperature and hydrostatic pressure permit the calculation of the temperature-induced change in refractive index at constant volume according to the equation,

$$dn/dT=\left[\rho\left(\frac{\partial n}{\partial\rho}\right)_T\frac{1}{\rho}\left(\frac{d\rho}{dT}\right)+\left(\frac{\partial n}{\partial T}\right)_\rho\right], \tag{16}$$

where ρ represents density. The term, $\frac{1}{\rho}\left(\frac{d\rho}{dT}\right)$, is equal to the negative of the volume coefficient of thermal expansion which, in turn, is equal to three times the linear coefficient of thermal expansion. The parameters, dn/dT and $(\partial n/\partial T)_\rho$, are important in calculating the thermal self-focusing of laser beams [32]. The first part of the laser pulse heats the glass and causes a change in the refractive index. dn/dT is important when there is sufficient time for thermal expansion of the glass to take place. In considering a Q-switched laser pulse which passes before the acoustic relaxation takes place, $(\partial n/\partial T)_\rho$ is the parameter of interest. Data on $\rho\left(\frac{\partial n}{\partial\rho}\right)_T$ are needed to calculate the self-focusing induced by electrostriction [33]. Calculations of $\frac{1}{\rho}\left(\frac{d\rho}{dT}\right)$, $\rho\left(\frac{\partial n}{\partial\rho}\right)_T$, $\frac{dn}{dT}$ and $\left(\frac{\partial n}{\partial T}\right)_\rho$ have been made for the five neodymium-doped laser glasses at 25 °C and the results are presented in table 7.

TABLE 7. *Parameters for calculating self-focusing of laser light in neodymium-doped laser glasses at 0.6438 μm at 25 °C*

	A	B	C	D	E
$\frac{1}{\rho}\left(\frac{d\rho}{dT}\right)\times10^6$	−29.4/°C	−30.1	−26.5	−29.0	−25.2
$\rho\left(\frac{\partial n}{\partial\rho}\right)_T$	0.34	0.34	0.34	0.36	0.30
$\frac{dn}{dT}\times10^6$	−1.8/°C	−1.6	−0.3	−4.0	2.8
$\left(\frac{\partial n}{\partial T}\right)_\rho\times10^6$	8.2/°C	8.6	8.7	6.4	10.3

9. Thermal Conductivity

The thermal conductivity measurements [34] were carried out on a sample cut from specimen E in the apparatus in figure 11. This apparatus utilizes a steady-state longitudinal heat flow method in which the electrically generated heat input to the specimen heater (A) flows perpendicularly from both sides of the heater through the specimens (B) to the cold plates (C). The average thermal conductivity of the two specimens was determined from the measured power to the heater, the measured temperature drops in the two specimens, and the geometry.

Measurements were made between 0 and 100 °C on a section cut from the cylindrical specimen. Since there appeared to be a discrepancy between the first set of measurements and the values obtained independently in another laboratory, a second set of measurements were made. The largest difference between the measurements at the same point was 1.1 percent, and this was well within the expected error of about 2 percent. A parabola was fitted to the data, and the results for the smoothed thermal conductivity values at 0, 50, and 100 °C are shown in table 8.

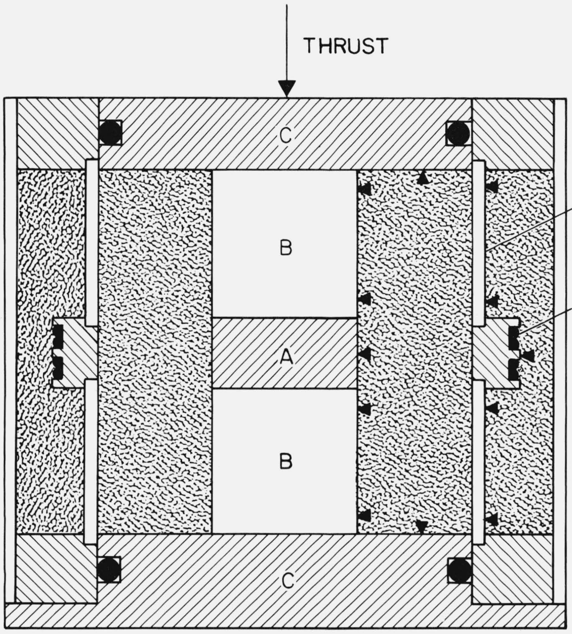

FIGURE 11. *Apparatus for measuring thermal conductivity.*
A, heater; B, specimens; C, cold plates; D, coaxial guard cylinder; E, guard heater.

TABLE 8. *Thermal conductivity of neodymium-doped laser glass, sample E*

Temperature, °C	Thermal conductivity $Wm^{-1}\,°C^{-1}$
0	1.19_7
50	1.29_0
100	1.34_8

10. Knoop Hardness

It is important that laser glasses have sufficient hardness to accept and retain good optical surfaces. The Knoop Hardness values for two of the glass specimens (B and E) were measured with indenting loads of 25, 50, 100, and 200 gram-force. The measuring microscope had a 4.0 mm objective, 0.85 N.A. (numerical aperture), and a 12.5X filar ocular [35]. The hardness tester was a MO Tukon, dash-pot rate at indenter, 0.2 mm/min. The indenter was a Wilson Knoop, No. 2054, with $C_p = 0.7060 \times 10^{-1}$. The Knoop Hardness values were read from a table containing a correction for the Abbe resolution error [35]. The values for the glasses are given in table 9.

TABLE 9. *Knoop hardness values for two neodymium-doped laser glasses*

Glass B

Observation	Indenting Load, gram weight			
	25	50	100	200
1	491	482	457	431
2	476	482	467	438
3	476	482	441	435
4	459	453	457	443
5	466	474	467	426
6	484	474	462	438
7	456	482	458	428
8	466	478	436	440
9	443	465	453	423
10	459	474	430	438
Average	467.6	474.6	452.8	434.0
0.6745 S.D.	3.1	2.0	2.7	1.4

Glass E

Observation	Indenting Load, gram weight			
	25	50	100	200
1	627	545	575	537
2	622	557	564	552
3	622	557	585	550
4	622	454	553	544
5	611	567	569	537
6	587	590	557	543
7	550	567	569	543
8	611	577	540	543
9	611	477	562	543
10	596	590	562	544
Average	605.9	567.2	563.6	543.6
0.6745 S.D.	5.0	3.5	2.6	1.0

Note 1 – Indentations were spaced at 0.5 mm intervals for Glass B and at 1 mm intervals for Glass E.
Note 2 – S.D. is the standard deviation of the mean.

11. Density

The density of samples from each of the five glasses was determined by the well known buoyancy method [36] using distilled water as the immersion liquid. The values for the five neodymium-doped glasses are given in table 10, where the limit of reproducibility is estimated to be 3 in the fourth decimal place.

TABLE 10. *Density of neodymium-doped laser glasses*

Glass	Density, g/cm^3
A	2.6012
B	2.6206
C	2.5935
D	2.5996
E	2.5490

12. Chemical Composition

Chemical analyses were made on samples from each of the five laser glasses. A preliminary general spectrochemical analysis was conducted to determine the elements present. The results are given in table 11. From this table it is seen that all of the glasses are silicates and that Glass A, B, C, and D are mixed alklai glasses. Glass E is different in that it contains a single alkali, lithium.

On the basis of the preliminary spectrochemical analysis, determinations of glass composition with respect to individual elements were made, classing those elements indicated to be at the 0.1 to 1 percent level or higher as major constituents. Table 12 summarizes the pertinent analytical data on the major constituents of the five laser glasses, along with the analytical methods employed in each case. The errors in the values of the major constituents of the glasses are estimated to be no greater than ± 1 in the last significant figure. The trace amounts of Fe_2O_3 found in the glasses are reported in this table because the absorption in the vicinity of the lasing wavelength is usually attributed to the Fe_2O_3 content. These values are believed to have a relative precision of ± 20 percent.

Neutron activation analyses were also made on a sample of each of the glasses, primarily to determine trace impurities, but also as a check on other methods. The results obtained are given in table 13. Here, again, the errors in the values of the major constituents are

TABLE 11. *Spectrochemical analyses of neodymium-doped laser glasses, weight percent*

Element	Glass A	Glass B	Glass C	Glass D	Glass E
Ag	–	–	–	–	–
Al	1–10	1–10	0.1–1	0.1–1	1–10
As	–	–	–	–	–
Au	–	–	–	–	–
B	–	–	<.001	<.001	<.001
Ba	1–10	1–10	1–10	1–10	0.001–0.01
Be	–	–	–	–	–
Bi	–	–	–	–	–
Ca	0.01–0.1	0.01–0.1	0.01–0.1	0.01–0.1	1–10
Cd	–	–	–	–	–
Ce	–	–	–	–	–
Co	–	–	–	–	–
Cr	–	–	–	–	–
Cs	?	?	–	–	–
Cu	<.001	<.001	<.001	<.001	–
Fe	.001–.01	.001–.01	.001–.01	.001–.01	.001–.01
Ga	–	–	–	–	–?
Ge	–	–	–	–	–
Hf	–	–	–	–	–
Hg	–	–	–	–	–
In	–	–	–	–	–
K	1–10	1–10	1–10	1–10	<.001
La	–	–	–	–	–
Li	.1–1	.1–1	<.001	<.001	1–10
Mg	<.001	<.001	<.001	<.001	<.001
Mn	–	–	–?	–?	–?
Mo	–	–	–	–?	–
Na	1–10	1–10	1–10	1–10	.01–.1
Nb	–	–	–	–	–
Nd	1–10	1–10	1–10	1–10	1–10
Ni	–	–	–	–	–
Os	–	–	–	–	–
Pb	–	–	1–10	1–10	–
Pt	–	–	–	–	–
Rb	.001–.01	.001–.01	.001–.01	.001–.01	–
Sb	.1–1	.1–1	.1–1	1–10	–
Si	>10	>10	>10	>10	>10
Sr	–	–	–	–	–?
Ta	–	–	–	–	–
Th	–	–	–	–	–
Ti	.1–1	.1–1	.1–1	.1–1	–
U	–	–	–	–	–
V	–	–	–	–	–
W	–	–	–	–	–
Zn	–	–	–	–	–
Zr	–	–	–	–	–

TABLE 12. *Major constituents of neodymium-doped laser glasses, weight percent*

Oxide	Glass A	Glass B	Glass C	Glass D	Glass E	Method
SiO_2	66.6	61.3	67.8	66.3	66.1	Gravimetric
Li_2O	1.0	1.0			14.5	Flame Emission Spectrometry
Na_2O	6.7	6.2	7.9	3.4		Flame Emission Spectrometry
K_2O	10.0	17.2	13.8	18.2		Flame Emission Spectrometry
CaO					10.1	Flame Emission Spectrometry
BaO	5.5	3.0	3.3	3.5		Flame Emission Spectrometry
PbO			1.1	1.8		Atomic Absorption Spectrometry
ZnO	1.6	1.8				Atomic Absorption Spectrometry
Al_2O_3	1.8	1.9			4.4	Flame Emission Spectrometry
Nd_2O_3	5.4	5.8	5.5	3.5	3.4	Spectrophotometry
Sb_2O_3	0.8	0.8	.9	3.2		Atomic Absorption
CeO_2					0.5	Neutron Activation
Fe_2O_3	0.011	0.010	0.0070	0.0090	0.0055	Spectrophotometry
TiO_2			0.19	0.39		Spectrophotometry
	99.4	99.0	100.3	99.9	99.0	

TABLE 13. *Neutron activation analyses of neodymium-doped laser glasses, weight percent*

Oxide	Glass A	Glass B	Glass C	Glass D	Glass E
Na_2O,	6.85	6.39	7.83	3.19	0.044
K_2O	9.21	17.1	13.8	16.6	< 0.04
Sb_2O_3	0.90	0.93	0.86	2.54	0.0015
Nd_2O_3	5.52	5.73	5.84	3.53	3.52
BaO	5.06	2.83	3.27	3.46	< 0.3
CeO_2	< 0.006	< 0.006	< 0.005	< 0.006	0.52
Parts per million					
La_2O_3,	< 0.9	7.8	10.2	17.8	< 0.8
Pr_2O_3	< 3	8.4	< 3	< 3	< 2
Eu_2O_3	29.7	1.1	0.6	≤ 0.1	< 0.5
Sm_2O_3	0.37	2.2	0.2	0.2	0.03

estimated to be no greater than ±1 in the last significant figure. For the amounts reported in parts per million, the standard deviation is estimated to be about ±5 percent in most cases. For the lower reported values of Sm there is severe interference from Nd and these values are probably no better than ±20 percent. For the lower reported values for Eu and Ce the signal-to-background ratio was poor and these values also are probably no better than ±20 percent. All results are reported as the oxide rather than the element to facilitate comparison with results from other methods.

13. Summary

As an aid in laser design, measurements have been made on important physical and chemical properties of five commercially available, neodymium-doped laser glasses. The measurements include thermo-optic properties, photoelasticity, refractive index, optical homogeneity, transmittance, thermal conductivity, hardness, density, and chemical composition. Calculations have been made of the thermal change in refractive index at constant volume, because this parameter is important in the study of self-focusing of laser light.

The combined facilities of the Inorganic Materials, Optical Physics, Polymers, Building Research, Mechanics and Chemistry Divisions within the National Bureau of Standards were utilized for making the measurements and compiling the data included in this report. The authors acknowledge the contribution of colleagues as follows: F. W. Rosberry for measurements of homogeneity, G. Dickson for determining the elastic constants, A. Feldman and D. Horowitz for determining the wavelength variation of the stress-induced birefringence, D. Flynn and W. L. Carroll for measurements of thermal conductivity, E. G. Hawkins for density measurements and D. R. Tate for determining the Knoop hardness. In addition, the workers who collaborated in making the chemical analyses were B. A. Thompson, B. B. Bendigo, T. A. Rush, T. C. Rains, E. R. Deardorff, and V. C. Stewart.

14. References

[1] Quelle, F. W., Jr., Appl. Optics **5**, 633 (1966).
[2] Blume, A. E., and Tittel, K. F., Appl. Optics **3**, 527 (1964).
[3] Sims, S. D., Stein, A., and Roth, C., Appl. Optics **5**, 621 (1966).
[4] Sims, S. D., Stein, A., and Roth, C., Appl. Optics **6**, 579 (1967).
[5] Epstein, S., J. Appl. Phys. **38**, 2715 (1967).
[6] Baldwin, G. D., and Riedel, E. P., J. Appl. Phys. **38**, 2726 (1967).
[7] Dishington, D. H., Hook, W. R., and Hilberg, R. P., Proc. IEEE **55**, 2038 (1967).
[8] Welling, H., and Bickart, C., J. Opt. Soc. Amer. **56**, 611 (1966).
[9] Guiliano, C. R., Appl. Phys. Letters **5**, 137 (1964).
[10] Chiao, R. Y., Townes, C. H., and Stoichéff, B. P., Phys. Rev. Letters **12**, 592 (1964).
[11] Olness, D., J. Appl. Phys. **39**, 6 (1968).
[12] Davit, J., J. Appl. Phys. **39**, 6052 (1968).
[13] Thornton, J. R., Fountain, W. D., Flint, G. W., Crow, T. G., Appl. Optics **8**, 1087 (1969).
[14] Snitzer, E., Appl. Optics **5**, 1487 (1966).
[15] Military Specification, Glass, Optical, MIL–G–174A, 5 Nov. 1963.
[16] Rosberry, F. W., Appl. Optics **5**, 961 (1966).
[17] Rogers, A. F., and Kerr, P. F., Optical Mineralogy (McGraw-Hill Book Co., Inc., New York and London, 1942).
[18] Weir, C., Spinner, S., Malitson, I. H., Rodney, W., J. Res. Nat. Bur. Stand. (U.S.), **58**, 189–194 (April 1957) RP2751.
[19] Rodney, W. S., and Spindler, R. J., J. Res. Nat. Bur. Stand. (U.S.), **53**, 185–189 (Sept. 1954) RP2531.
[20] Tilton, L. W., J. Res. Nat. Bur. Stand. (U.S.), **2**, 909–930 (1929) RP64.
[21] Dodge, M. J., Malitson, I. H., and Mahan, A. I., Appl. Opt. **8**, 1703 (1969).
[22] Private communication. L. E. Sutton, Institute of Basic Standards, National Bureau of Standards, Washington, D.C.
[23] Saunders, J. B., J. Res. Nat. Bur. Stand. (U.S.), **35**, 157–218 (Sept. 1945) RP 1668.
[24] Krishnan, R. S. Progress in Crystal Physics, Vol. **I** (Interscience Publishers, New York and London, 1958).
[25] Ramachandran, G. N., Proc. Ind. Acad. Sci. [A] **25**, 498 (1947).
[26] Ramachandran, G. N., Proc. Ind. Acad. Sci. [A] **25**, 286 (1947).
[27] Waxler, R. M., and Weir, C. E., J. Res. Nat. Bur. Stand. (U.S.), **69A**, (Phys. and Chem.), No. 4, 325–333 (July–Aug. 1965).
[28] Waxler, R. M., and Napolitano, A., J. Res. Nat. Bur. Stand. (U.S.), **59**, 121–125 (Aug. 1957) RP 2779.
[29] Feldman, A., Phys. Rev. **150**, 748 (1966).
[30] Vedam, K., Proc. Ind. Acad. Sci. [A] **31**, 450 (1950).
[31] Dickson, G., and Oglesby, P. L., J. Dent. Res. **46**, [6] Part 2, 1475 (1967).
[32] Quelle, F. W., Damage in Laser Glass, ASTM STP 469 (American Society for Testing and Materials, 1969) pp. 110–116.
[33] Kerr, E. L., IEEE J. Quantum Electronics **QE–6**, 616 (1970).
[34] Wachtman, J. B., Jr., Mechanical and Thermal Properties of Ceramics, Nat. Bur. Stand. (U.S.), Spec. Publ. 303, 272 pages (May 1969).
[35] Brock, T. W., Draft of Tentative Method of Test for Knoop Indentation Hardness of Glass. Being considered for approval as an ASTM method by ASTM Committee C14.04.
[36] Glaze, F. W., Young, J. C., and Finn, A. N., J. Res. Nat. Bur. Stand. (U.S.), **9**, 799–805 (1932) RP 507.

(Paper 75A3–660)